Available online at www.sciencedirect.com
SCIENCE DIRECT®
PHOTONICS AND NANOSTRUCTURES
Fundamentals and Applications
ELSEVIER
Photonics and Nanostructures – Fundamentals and Applications xxx (2006) xxx–xxx
www.elsevier.com/locate/photonics

Omni-reflectance and enhanced resonant tunneling from multilayers containing left-handed materials

H. Daninthe [a,b], S. Foteinopoulou [a,c,*], C.M. Soukoulis [a]

[a] *Ames Laboratory-USDOE and Department of Physics and Astronomy, Iowa State University, Ames, IA 50011, USA*
[b] *Theoretical Physics and Modelization Laboratory, CNRS-Cergy-Pontoise University (UMR 8089), F-95031 Cergy-Pontoise Cedex, France*
[c] *Laboratoire de Physique du Solide, Facultès Universitaires Notre-Dame de la Paix, Rue de Bruxelles 61, B-5000 Namur, Belgium*

Received 23 October 2005; received in revised form 12 January 2006; accepted 12 January 2006

Abstract

We study the oblique transmission through a one-dimensional photonic crystal consisting of alternating slabs made of ordinary and negative refractive index materials, the latter being dispersive. We investigate the angular dependence of the band gap for this multilayer medium. Our results suggest, unlike a conventional Bragg gap, this type of gap exhibits a rather versatile behavior with varying angle of incidence. We find the angle-dependent characteristics for this type of gap can be quite different for different structural parameters of the constituents. Thus, multilayer structures involving left-handed components are very good candidates for band gap engineering. Specifically, we demonstrate for a certain experimentally realizable structure, the existence of a gap region for each individual polarization which survives for incident angles as high as 85 °. Moreover, we show how this structure can also function as a highly efficient polarization splitter. Finally, we investigate the multilayer medium when acting as single or double electromagnetic barrier. We study the tunneling properties of such systems for both types of individual barrier layers—right- and left-handed, respectively. We observe the double barrier exhibits resonant tunneling that depends on the ''rightness'' of the individual barrier layers.

PACS: 42.70.Qs; 41.20.Jb; 78.20.Ci

Keywords: Left-handed materials; Backwards wave; Omnigap; Multilayers; Tunneling

1. Introduction

Veselago [1] first explored in 1967 the possibility of EM wave propagating in a medium with simultaneously negative permittivity, ε, and permeability, μ. Such a medium came to be known as left-handed (LHM), since it has the wave vector **k**, the electric field vector **E**, and the magnetic field vector **H** forming a left-handed (LH) set of vectors. Veselago also predicted that a LHM possesses many unusual properties such as negative refraction, backwards wave propagation, reversed Doppler effect, etc. Recently, the UCSD group [2] brought this medium to realization with a man-made composite, which consists of metallic split ring resonators (SRR) and wires. This composite was shown to possess a frequency window where the effective permittivity, ε_{eff}, and permeability, μ_{eff}, are simultaneously negative [3–6]. These types of metamaterials have a refractive index, $n = -\sqrt{\varepsilon\mu}$ [1] and are also commonly referred to as double negative materials (DNG). Left-handed materials and their unusual properties are attracting increasing attention in view of their vast potential for many applications. Many other composite metallic designs that possess these unusual

* Corresponding author. Tel.: +3281724704; fax: +3281724707.
E-mail address: sfoteino@fundp.ac.be (S. Foteinopoulou).

1569-4410/$ – see front matter © 2006 Elsevier B.V. All rights reserved.
doi:10.1016/j.photonics.2006.01.001

properties have been explored [7,8]. Recently, negatively refractive phenomena were also studied in periodic dielectric structures (photonic crystals) [9–12].

The band gap properties of conventional photonic crystals (PCs) [13] have been extensively studied. Nonetheless, double negative materials in a periodic arrangement were investigated only recently [14]. Specifically, Li et al. studied a one-dimensional periodic medium, consisting of alternating double negative slabs and air. They identified the existence of a band gap around a frequency which corresponds to a zero average refractive index, n_{av} [15]. They found that this band gap does not depend on the structural parameters, provided the $n_{av} = 0$ condition is observed at the same frequency. Actually, such a behavior is very different from conventional PCs. This study directed a lot of attention towards multilayer structures involving left-handed components [16–20]. In addition, other researchers [21,22] explored multilayer systems, where the alternating slabs consist of negative permittivity, ε, and permeability, μ, respectively.

In this paper, we study the transmission of EM waves through a multilayer structure consisting of alternating double negative slabs and a positive index medium. We focus on the behavior of the transmission with the angle of incidence for both polarizations and investigate the possibility of omni-reflectance [23]. Moreover, we study the tunneling properties of a single and double barrier EM system. Of particular interest are cases where the barrier layers are made from a double negative (left-handed) medium. In particular, this study is divided in the following way. We present the theoretical formulation of the wave transmission through a general superlattice in Section 2. In Section 3, we implement the particular case, where one of the layers is a double negative medium, and study the dependence of the gap with the angle of incidence for both polarizations. In Section 4, we focus on a multilayer system consisting only of one or two double negative layers embedded in air, for cases when the propagation is prohibited inside the individual layers. We investigate the tunneling properties for the left-handed barrier problem and make a comparison with a corresponding ''right-handed'' system. Finally, we present our conclusions in Section 5.

2. Theoretical formulation of the problem

We show the one-dimensional multilayer system under study in Fig. 1. The specifics for the two polarizations are shown in Fig. 1 a and b, respectively. Note, with TE we mean that the electric field vector is

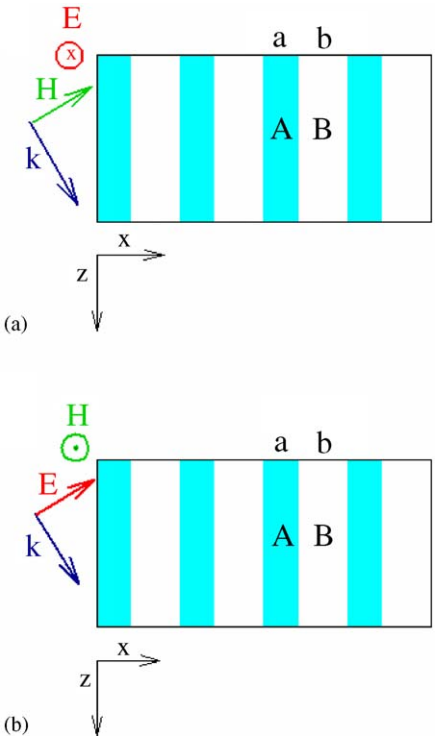

Fig. 1. The 1D multilayer system consisting of layers A and B in periodic arrangement. a and b represent the dimensions of layer A and B, respectively. Thus, the multilayer has a lattice constant, $d = a + b$. Case (a) represents the case of TE polarization, while case (b) represents the case of TH polarization. Note, for normal incidence, the two polarizations are equivalent. The multilayer composite is embedded in a medium identical with layer B.

perpendicular to the plane of incidence. Conversely, in TH polarization the magnetic field is perpendicular to the plane of incidence. We choose z to represent the lateral direction, and x the stacking direction (see Fig. 1). We consider N bilayers, i.e., a total number of $2N$ layers. Let ε_A, ε_B be the permittivity of layers A and B, respectively. Correspondingly, μ_A, μ_B represent the permeabilities of the two layers. The formulas we present in the following are general, provided the following restrictions apply. The EM waves must be incident and collected in a medium identical to medium B. Medium B must have real permittivity ε_B and permeability μ_B, with $\varepsilon_B\mu_B > 0$. Medium A must have ε_A and μ_A real.

Let us consider a monochromatic plane wave hitting the structure from the left, with an angle θ_B. The wave vector inside layer A(B) $\mathbf{k}_{\mathbf{A(B)}}$ is given as

$$k^2_{A(B)} = \frac{\omega^2}{c^2} n^2_{A(B)} = k^2_{A(B)x} + \beta^2. \quad (1)$$

$n_{A(B)} = \text{sign}(r_{A(B)})\sqrt{\varepsilon_{A(B)}\mu_{A(B)}}$ represents the refractive index of mediums A and B, respectively. $\text{sign}(r_{A(B)})$ represents the sign of the rightness for layers A(B). So, this sign is (+) for a right-handed and (−) for a left-handed layer. The quantity, $\beta = n_B\omega/c\sin\theta_B$ [24], is real. It represents the parallel component of the wave vector and, consequently, is conserved throughout the multilayer. However, depending on the incident angle and the values of ε_A, μ_A, the normal component of the wave vector in layer A, k_{Ax}, can be real or purely imaginary.

We treat each polarization separately.

Let, $\vec{F}(\vec{r};t) = \hat{y}F(x)e^{-i\omega t+i\beta z}$ with

$$F(x) = \begin{cases} c_0 e^{-ik_{Bx}x} + d_0 e^{ik_{Bx}x}, x \le 0 \\ a_m e^{-ik_{Ax}(x-md)} + b_m e^{ik_{Ax}(x-md)}, x \in A(m) \\ c_m e^{-ik_{Bx}(x-md-a)} + d_m e^{ik_{Bx}(x-md-a)}, x \in B(m) \\ a_t e^{-ik_{Bx}(x-Nd)} + b_t e^{ik_{Bx}(x-Nd)}, Nd \le x. \end{cases} \quad (2)$$

In Eq. (2)(a_t, b_t) characterize the field, F, in the region after the multilayer system. Note, F represents the electric field, E_y, for the case of TE polarization (s-waves) and the magnetic field, H_y, for the case of TH polarization (p-waves). For each case, we use Maxwell's equation to determine the remaining field components. Subsequently, we apply the continuity of the tangential components of $\vec{E}$ and $\vec{H}$ at the boundary between two layers.

In this way, we obtain the field values at $x = 0(-)$, in terms of the field values at $x = Nd(+)$. We express such a relation in matrix form. The resulting matrix is generally referred to as the transfer matrix. Afterward, we impose the Bloch condition, $E(x+d) = e^{iqd}E(x)$, for the periodic multilayer. Note, q lies within the first Brillouin zone, namely $-\pi/d \le q \le \pi/d$. We obtain q from the eigenvalues of the transfer matrix corresponding to one single bilayer. Let us define, $Z_{A/B} = (k_{Ax}/\mu_A)/(k_{Bx}/\mu_B)$ and $Y_{A/B} = (k_{Ax}/\varepsilon_A)/(k_{Bx}/\varepsilon_B)$. We get,

$$\cos(qd) = \cos(k_{Ax}a)\cos(k_{Bx}b) - \frac{1}{2}(Z_{A/B} + Z_{B/A})\sin(k_{Ax}a)\sin(k_{Bx}b), \quad (3)$$

for the TE-polarization and

$$\cos(qd) = \cos(k_{Ax}a)\cos(k_{Bx}b) - \frac{1}{2}(Y_{A/B} + Y_{B/A})\sin(k_{Ax}a)\sin(k_{Bx}b), \quad (4)$$

for the TH polarization. Note, $Z_{A/B}$, $Z_{B/A}$ and k_{Ax} can be imaginary in Eqs. (3) and (4). Nonetheless, when the conditions we stated earlier in this section are met, the properties of the transfer matrix lead to a real $\cos(qd)$.

We use Chebyshev's identity [25] to evaluate the transfer matrix for the total structure consisting of N bilayers. The calculation yields for the total transmission T:

$$T = \frac{1}{1 + |(r/t)|^2 |(\sin(Nqd)/\sin(qd))|^2}, \quad (5)$$

with

$$\frac{r}{t} = \begin{cases} \frac{i}{2}(Z_{B/A} - Z_{A/B})\sin(k_{Ax}a)e^{ik_{Bx}b} & \text{TE} - \text{pol} \\ \frac{i}{2}(Y_{B/A} - Y_{A/B})\sin(k_{Ax}a)e^{ik_{Bx}b} & \text{TH} - \text{pol}. \end{cases} \quad (6)$$

In Eq. (6)$r(t)$ represents the reflection (transmission) coefficient through a single unit cell.

3. Omnidirectional gap

For consistency and comparison with the results of Li et al. [14], we adopt a multilayer with the same structural parameters as in [14]. Specifically, we consider layer A to have permittivity and permeability given by,

$$\varepsilon_A(f) = 1 + \frac{5^2}{0.9^2 - f^2} + \frac{10^2}{11.5^2 - f^2}, \quad \mu_A(f) = 1 + \frac{3^2}{0.902^2 - f^2} \quad (7)$$

where f is the frequency measured in GHz. As frequency increases, we move from cases with both ε_A, μ_A negative (region I), to cases with $\varepsilon_A\mu_A < 0$ (region II), and eventually to cases with both ε_A and μ_A positive (region III). In Fig. 2 we plot the permittivity and permeability of layer A versus frequency. Cases with frequencies in region I (see Fig. 2), are of particular interest, since layer A becomes a double negative (DNG) medium. Note, a DNG medium must be dispersive to assure positive definite energy density [1]. For layer B we choose vacuum with $\varepsilon_B = \mu_B = 1$.

First, we concentrate on the TE-polarization case, and take the dimensions of the two layers (a and b) to be 6 and 12 mm, respectively. We plot transmission versus frequency for normal incidence in Fig. 3. Note, the first gap is centered around 2.3 GHz. This frequency value corresponds to an average refractive index, $n_{av} = 0$ [14,15]. We stress, in the frequency region of the first gap, layer A has both ε_A and μ_A negative. Nonetheless, in the frequency region of the second gap, layer A has

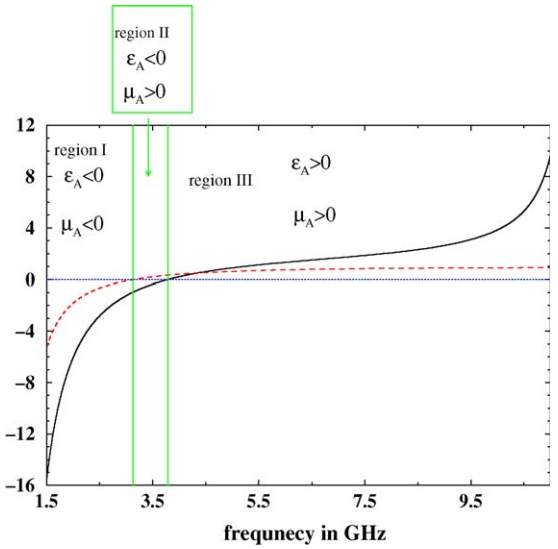

Fig. 2. Permittivity (solid line) and permeability (dashed line) of layer A versus frequency.

both ε_A and μ_A positive and is therefore an ordinary positive index medium. The second gap is a Bragg type gap, well familiar from photonic crystals and conventional Bragg reflectors [26]. We find this gap shifts in frequency, as the incident angle varies as expected. However, it is interesting to check how the first gap behaves for different incident angles. We show the results for this gap in Fig. 4. Strikingly, we observe that the location of the gap remains the same, even for an incident angle as large as 80°. In other words, the gap in the frequency region where layer A is left-handed, is an omni-gap.

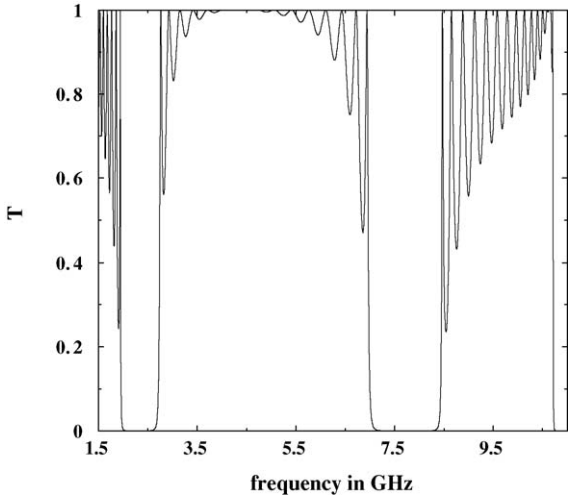

Fig. 3. Transmission vs. frequency for the multilayer system of Fig. 1 (TE-polarization). Layer A has permittivity and permeability given by (7) and length $a = 6$ mm. Layer B is air, and has length $b = 12$ mm.

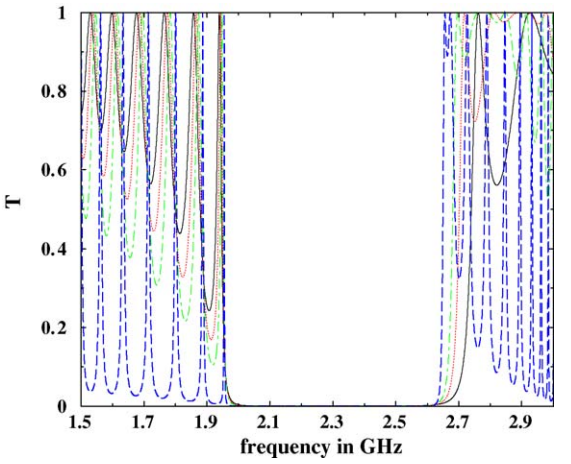

Fig. 4. Dependence of the first gap seen in Fig. 3 with angle of incidence θ_B. Solid, dotted, dot-dashed and dashed line represent $\theta_B = 0$, 30, 45 and 80°, respectively. Note, in this frequency range, layer A is a double negative (DNG) medium.

We find that the same structure for the TH polarization does not possess such a type of omni-gap. However, if we reverse the dimensions a and b of the multilayer system, we obtain an omni-gap for the TH polarization case as well. Fig. 5 shows such a case, with the dimensions of the constituent layers, $a = 12$ mm and $b = 6$ mm, respectively. Notice again, that the band gap survives even for very large angle of incidence (80°).

We note at this point that Jiang et al. [18] have identified the existence of an omnigap for both

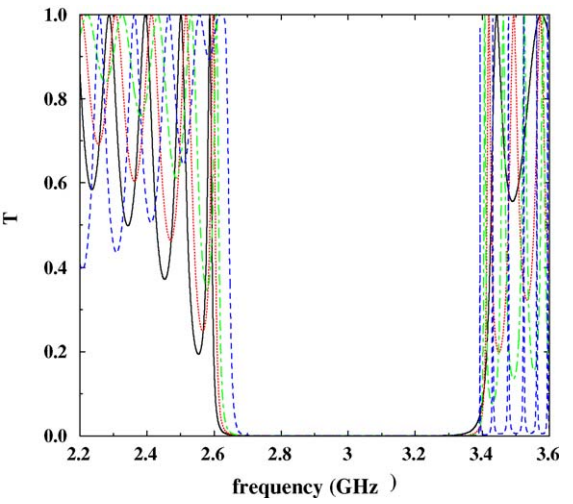

Fig. 5. Transmission vs. frequency for the system of Fig. 1 (TH-polarization), for different incident angles, θ_B. In this case, $a = 12$ mm and $b = 6$ mm. Solid, dotted, dot-dashed and dashed lines represent $\theta_B = 0, 30, 45$ and 80°, respectively. We observe the existence of the omni-gap.

polarizations around the frequency where the average refractive index, n_{av}, equals 0 [15]. The 1D layered system of Jiang et al. consists of left-handed slabs, which alternate with slabs having a refractive index of 2. The left-handed layers have permittivity and permeability, following a plasma like dispersion. We investigate further the gap properties of such a system, but have substituted the positive index layer with a material having a lower refractive index of $\sqrt{2}$ [27]. For such a multilayer medium, the $n_{av} = 0$ condition is satisfied for a higher frequency (at $f = 0.80$ GHz versus 0.70 GHz for the original system of Jiang et al. [18]). We found that if the refractive index of the right-handed layer is reduced to $\sqrt{2}$, then only the omnigap for the TH-polarization survives. As a matter of fact, for the TE-polarization as the angle of incidence increases from 0 to 89°, only 30% of the normal incidence gap continues to lie within the oblique incidence gap region. In other words, we do not observe an angle insensitive omnigap. Also, we find that for this modified structure, a higher number of bilayers is required to achieve the same transmission attenuation within the gap region. Now, we further modify this system by changing the dimensions of the constitutive layers. In particular, we take both layers to have the same size of 9 mm, thus maintaining the same lattice constant. For the resulting multilayer system, the $n_{av} = 0$ condition is satisfied at ~ 1.0 GHz. For this case we find that the lower frequency limit of the TE-polarization gap closes $\sim 35\%$ as the angle of incidence increases from 0 to 89°. Conversely, we find that the upper frequency limit of the TH-polarization gap closes $\sim 40\%$ as the angle of incidence increases from 0 to 89°.

These results indicate that contrary to the conclusion of Jiang et al. [18], the $n_{av} = 0$ condition does not necessarily guarantee the existence of an angle insensitive omnigap for either or both polarizations. Multilayer structures involving LHM can be experimentally realized at the microwave regime by incorporating composite SRR/wire structures. The latter composite media are characterized by an effective permittivity following a plasma-like dispersion and an effective permeability following a Lorentz type dispersion. We focus on a specific realistic system, incorporating the composite SRR/wire medium studied by Markos and Soukoulis [4]. We use the effective medium parameters determined in Ref. [4] to treat this medium, but ignore dissipation. So,

$$\varepsilon_A = 1 - \frac{19^2}{f^2}, \tag{8}$$

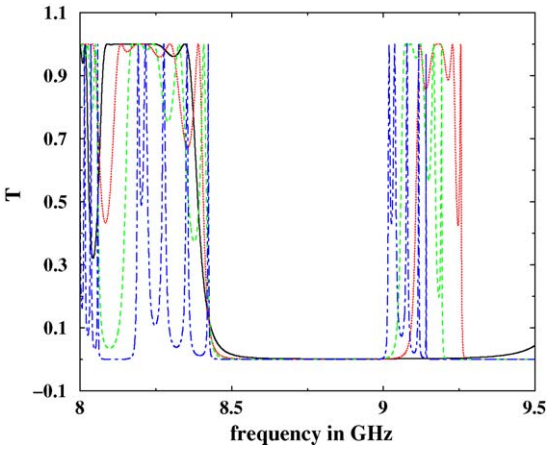

Fig. 6. Transmission vs. frequency for a realistic multilayer medium, for different incident angles θ_B. In this case, $a = 5$ mm and $b = 10$ mm. Solid, dotted, dot-dashed, and dashed lines represent $\theta_B = 0, 30, 45$ and 85°, respectively. We observe a gap region between 8.5 and 9.0 GHz surviving for incident angles as high as 85°. The incoming wave is TE polarized.

$$\mu_A = 1 - \frac{0.3 f^2}{f^2 - 7.9^2}, \tag{9}$$

with f the frequency in GHz.

This composite medium possesses simultaneously negative permittivity and permeabilty for frequencies between ~ 8 and 9.4 GHz. We consider the left-handed slabs as wide as the unit cell of the composite medium, i.e., 5 mm wide. We take the positive index slabs to be air and 10 mm wide, and consider a total of 5 bilayers. As we see in Fig. 6, the region between ~ 8.5 and 9.0 GHz remains within the gap, even for incident angles as high as 85° for TE-polarized waves. Note, this region is not centered around ~ 8.56 GHz, where the $n_{av} = 0$ condition is met for this particular multilayer medium. We checked that for TH-polarized waves the regime between ~ 9.1 and 9.4 GHz lies inside the gap for all incident angles. Unfortunately, this frequency region does not overlap with that of the TE-polarization case. In other words, for this particular realistic structure, we obtain a frequency regime of omni-reflectance for each individual polarization but not for both polarizations at the same time.

We can utilize this differential behavior under polarization of such a multilayer medium for the design of an efficient polarization splitter. Actually, we consider the same system and incident waves at 60°. We plot the transmission results in Fig. 7, for TE- and TH-polarizations. These results imply that if a wave of mixed polarization hits the interface of the structure at 60°, ''almost all'' of the TE-polarized contribution will

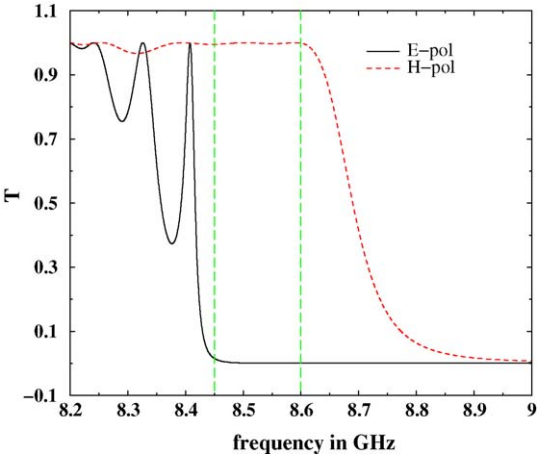

Fig. 7. A realistic multilayer structure, acting as a polarization splitter. Same parameters are taken as in Fig. 6. Waves are incident at 60°. Solid(dashed) line represents transmission for the case of TE(TH)-polarized waves. In a frequency window between ~8.45 and 8.6 GHz "almost all" TH-polarized wave is transmitted, while "almost all" TE-polarized wave is reflected.

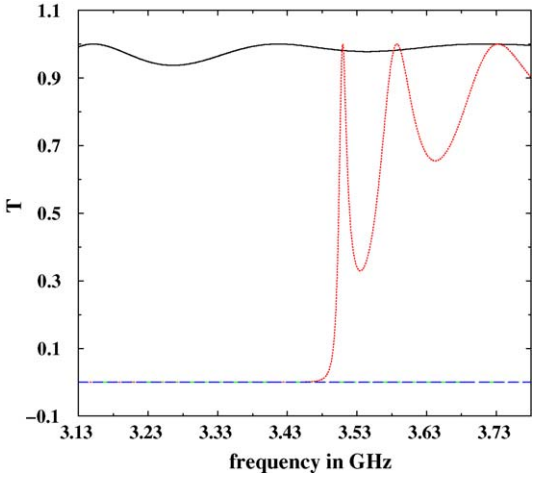

Fig. 8. Transmission versus frequency for the system of Fig. 1 (TE-polarization), for different incident angles θ_B. We focus on the frequency region from 3.13–3.78 GHz, where $\varepsilon_A\mu_A < 0$. In this case, $a = 6$ mm and $b = 12$ mm. Solid, dotted, dot-dashed and dashed lines represent $\theta_B = 0$, 30, 45 and 80°, respectively. Tunneling is stronger for the smaller angles. Note, the curves for $\theta_B = 45$ and 80° are around zero transmission and therefore one falls on top of the other.

be reflected while "almost all" of the TH-polarized contribution will be transmitted. In this way, efficient polarization splitting is achieved for the frequency region between ~8.45 and 8.6 GHz, as indicated in Fig. 7 with the dashed vertical lines.

To resume, multilayer structures involving left-handed components show enormous potential for band gap engineering and related applications. A region of omnireflectance can be usually obtained for at least one polarization even for realistic cases. However, we showed firm evidence that the $n_{av} = 0$ [15] condition does not necessarily lead to an angle insensitive omnigap for both polarizations, as indicated in the work of Jiang et al. [18].

4. Resonant tunneling phenomena

Another important point, in the case of Fig. 5, is that layer A remains left-handed only in part of the omni-gap. In fact, for a small window of frequencies ranging from 3.13 to 3.78 GHz, we have $\varepsilon_A < 0$, with $\mu_A > 0$. This means, that in the range from ~3.13–3.38 GHz, propagation is forbidden both in the individual layers A (imaginary k_{Ax}), and in the entire composite multilayer (imaginary q in Eq. (4)). Interestingly, in the frequency range between 3.38 and 3.78 GHz, although propagation in the individual layers A is still prohibited, propagation in the entire composite is allowed (real q in Eq. (4)).

The latter phenomenon is not unique for the TH-polarization case. In fact, there is a similar phenomenon for the structure of Fig. 1 (TE-polarization). Again, we focus on the frequency range between 3.13 and 3.78 GHz, where $\varepsilon_A < 0$, with $\mu_A > 0$ (region II of Fig. 2). We study the angle dependent transmission of the multilayer system and show our results in Fig. 8. Since $\varepsilon_A\mu_A < 0$, in this frequency range the wave vector along the stacking direction in layer A, k_{Ax}, becomes imaginary. Correspondingly, EM propagation is prohibited in the individual layers of medium A. Therefore, the high transmission we see in some cases in Fig. 8 suggests a tunneling type of effect. The phenomenon seems to depend highly on both the incident angle and structural parameters. By investigating different cases, we determined that the control parameter is $k_{Ax}a$. Let $k_{Ax} = i\lambda_{Ax}$. Then, we obtain

$$\lambda_{Ax} = \omega/c\sqrt{|\varepsilon_A\mu_A| + sin^2\theta_B}. \quad (10)$$

λ_{Ax} in Eq. (10) represents the decay rate of the field within the individual layers of medium A. We see that as the angle increases, λ_{Ax} increases. Correspondingly, the decay rate of the field within the layers of medium A increases and so the tunneling possibility decreases. This observation is consistent with the results shown in Fig. 8.

We proceed in exploring tunneling phenomena for cases having $\varepsilon_A\mu_A > 0$, with ε_A, μ_A given by Eq. (7). We limit ourselves to the left-handed region (region I in Fig. 2) and incident angles falling on or above the

total internal reflection (TIR) condition. This condition can be expressed as:

$$\beta \geq \sqrt{\varepsilon_A \mu_A}\omega/c, \tag{11}$$

for waves incident from medium B onto medium A. The equal sign represents the case of an EM wave falling exactly on the TIR condition. Since medium B is air, in order for Eq. (11) to be possible, the magnitude of the refractive index of layer A, n_A, must be less than 1. This can happen for certain frequencies lying within region I (see Fig. 1). When an incident wave falls exactly on the TIR condition, we see from Eq. (1) that k_{Ax} becomes 0. In such a case, an incident EM wave refracts along the lateral direction of a slab made of material A. Now, when an incident wave falls above the TIR condition, k_{Ax} becomes imaginary, implying that propagation is prohibited within layer A. In both cases, one would not expect an EM wave to get transmitted across the slab. In the following, we study an arrangement as seen in Fig. 2, with $N = 1$(one layer of medium A) and $N = 2$(two layers of medium A). The quantum mechanical analogue of this problem is a single or double barrier problem.

We search for resonant tunneling with $T = 1$ and record the corresponding frequency for different incident angles satisfying condition (11). We plot our results in Fig. 9. For certain characteristic angles, 70, 80 and 85°, we also plot the transmission versus frequency (within the TIR range) for the single (Fig. 10 a) and double (Fig. 10 b) barrier problem. We identify only one $T = 1$ resonance for the single barrier problem. On the other hand, two $T = 1$ resonances are present in the double barrier case. The location of the first resonance in the double barrier case coincides with the corresponding resonance in the single barrier case.

For cases when only one barrier is involved, ($N = 1$) transmission T becomes

$$T = \frac{1}{1 + |(r/t)|^2}, \tag{12}$$

while in the case of the double barrier transmission is

$$T = \frac{1}{1 + 4|(r/t)|^2 |\cos(qd)|^2}. \tag{13}$$

It can be easily deduced from Eqs. (12) and (13) that the common resonant peaks observed in the single and double barrier problem correspond to $r/t = 0$. This condition occurs only when k_{Ax} equals to zero [28,29]. Naturally, this case is not sensitive to the specifics of the barrier problem. In principle, it can

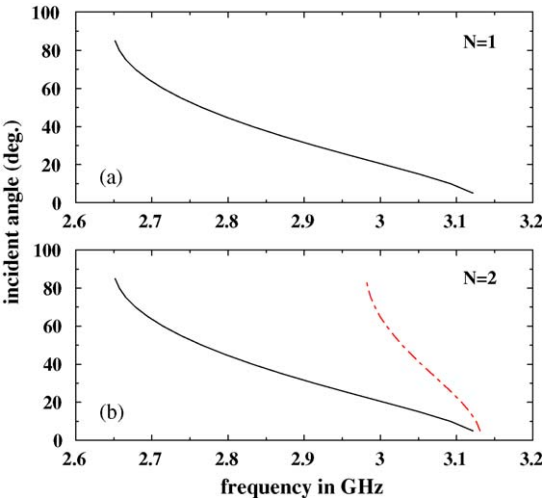

Fig. 9. Resonant tunneling for cases where layer A is DNG and the TIR condition is met. We plot the incident angle vs. the frequency location of the $T = 1$ resonant peaks. Top panel (a) refers to the single barrier problem ($N = 1$). Bottom panel (b) refers to the double barrier problem ($N = 2$).

be observed in any EM barrier problem at frequency and angle satisfying Eq. (11) with the equal sign. On the other hand the second set of $T = 1$ resonant peaks seen in Figs. 9 b and 10 b occurs when $\cos(qd) = 0$ in the double barrier problem. Evidently, we infer from Eq. (3) this type of resonances depend on many parameters, such as the size of the barriers, a, the distance between them, b, the values of permittivity, and permeability etc.

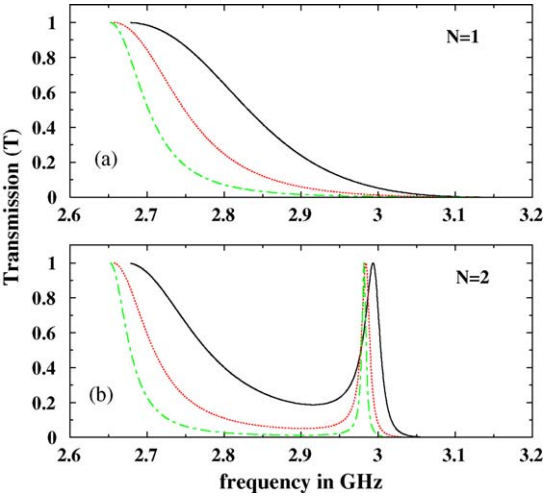

Fig. 10. Resonant tunneling peaks for cases where layer A is DNG and the TIR condition is met. We plot the transmission vs. the frequency for different incident angles: $\theta_B = 70°$ (solid line), $\theta_B = 80°$ (dotted line) and $\theta_B = 85°$ (dot-dashed line). Top panel (a) refers to the single barrier problem ($N = 1$). Bottom panel (b) refers to the double barrier problem.

It is of particular interest to understand the influence of the ''rightness'' of the barrier layer(s) on the resonant tunneling phenomenon. It is self evident that ''rightness'' has no impact on the resonant peaks arising from $r/t = 0$. However the ''rightness'' of the barrier layers does impact the value of $\cos(qd)$ and correspondingly the second type of resonant tunneling peaks. In order to understand this, we assign to layer A permittivity and permeability opposite in sign to the values given in Eq. (7). In fact, we find that the second type of resonant peaks disappear. We should not rush to the conclusion that the appearance of this sort of resonant tunneling peaks is unique to left-handed double barrier systems. In principle, by tuning the parameters appropriately this type of tunneling phenomenon can exist in conventional right-handed double barrier systems as well. Interestingly, however, if for certain parameters and polarization the left-handed barrier exhibits resonant tunneling of this sort, the corresponding right-handed barrier system will not possess a resonant tunneling peak at the same frequency location. The reverse statement also holds.

We explain why in the following. In the TIR region the normal wave vector component inside layer A, k_{Ax}, is purely imaginary. We set $k_{Ax} = ik_{Axp}$ in Eqs. (3) and (4). We obtain for the TE-polarization case

$$\cos(qd) = \cosh(k_{Axp}a)\cos(k_{Bx}b) + \frac{1}{2}\mathrm{sign}(\mu_A)\left(\frac{k_{Axp}/|\mu_A|}{k_{Bx}/\mu_B} - \frac{k_{Bx}/\mu_B}{k_{Axp}/|\mu_A|}\right) \times \sinh(k_{Axp}a)\sin(k_{Bx}b), \tag{14}$$

and for the TH-polarization case

$$\cos(qd) = \cosh(k_{Axp}a)\cos(k_{Bx}b) + \frac{1}{2}\mathrm{sign}(\varepsilon_A)\left(\frac{k_{Axp}/|\varepsilon_A|}{k_{Bx}/\varepsilon_B} - \frac{k_{Bx}/\varepsilon_B}{k_{Axp}/|\varepsilon_A|}\right) \times \sinh(k_{Axp}a)\sin(k_{Bx}b). \tag{15}$$

In Eqs. (14) and (15) k_{Axp} and k_{Bx} are real and positive. Suppose, a left-handed barrier satisfies the condition $\cos(qd) = 0$ for a certain frequency and parameters. Let us consider the corresponding right-handed barrier system for the same frequency and parameters. All will be the same in Eqs. (14) and (15) except for $\mathrm{sign}(\mu_A)$ and $\mathrm{sign}(\varepsilon_A)$, respectively. As a result for the right-handed system, $\cos(qd) \neq 0$, and correspondingly no resonant tunneling will occur. From Eqs. (14) and (15), we also deduce that if one desires a resonant tunneling peak of this sort for both polarizations, we must have $\varepsilon_A = \mu_A$ at the frequency of interest.

5. Conclusions

To summarize, we studied the angle dependent transmission properties of a layered medium, comprised of alternating negative and positive refractive index slabs. Around the frequency where n_{av} is zero [15], these types of multilayers are expected to possess unusual band gap properties independent on both angle and polarization [18]. For a certain type of constituent left-handed medium, we were able to identify an omni-gap of this type. However, we found such a behavior for each separate polarization, by modifying the structural dimensions appropriately. Moreover, further investigation of different structures contradicts the conclusion of Jiang et al. [18]. In particular, we have shown that the $n_{av} = 0$ condition does not necessarily lead to an angle insensitive omnigap for either or both polarizations. We have extended our study to multilayers that are experimentally realizable. This is possible in the microwave regime by incorporating metallic composite media with effective negative refractive index [4]. For the latter medium, we found a frequency region of omnireflectance – surviving for angles as high as 85° – for each separate polarization. We also showed how such a structure can function as a highly efficient polarization splitter.

In the second part of our work, we focused on the tunneling properties of a single and double layer systems, in the case where they act as EM barriers. We observed that resonant tunneling depends highly on the structural parameters of the system and polarization. Moreover, we find that the ''rightness'' of the barrier layers impacts the tunneling phenomenon in a unique way. Reversing the ''rightness,'' while keeping all other parameters the same will cause one of the peaks of the double barrier problem to appear, disappear or change frequency location.

Therefore, multilayers involving left-handed components show enormous promise for band gap engineering and related applications. The study of many more designs of effective left-handed media in the microwave regime will aid in this direction [7,8,17]. Moreover, a recent report for artificial magnetism at the THz regime [30] shows promise for scalability of these multilayer structures at higher frequencies. We believe this work will aid in the design of reflectors, polarization filters and splitters, beam deflectors etc.

Acknowledgments

H. Daninthe wants to thank the Department of Physics and Astronomy of Iowa State University, and Ames Laboratory for their hospitality. Ames Laboratory is operated by the U.S Department of Energy by Iowa State University under Contract No. W-7405-Eng-82.

References

[1] V.G. Vesalago, Usp. Fiz. Nank 92 (1964) 517;
V.G. Vesalago, Sov. Phys. Usp. 10 (1968) 509.
[2] R.A. Shelby, D.R. Smith, S. Shultz, Science 292 (2001) 77.
[3] J.B. Pendry, A.J. Holden, D.J. Robbins, W.J. Stewart, IEEE Trans. Microwave Theory Tech. 47 (1999) 2075.
[4] P. Markoš, C.M. Soukoulis, Phys. Rev B 65 (2002) 033401.
[5] P. Markoš, C.M. Soukoulis, Phys. Rev. E 65 (2002) 036622.
[6] D.R. Smith, S. Schultz, P. Markos, C.M. Soukoulis, Phys. Rev. B 65 (2002) 195104.
[7] C.G. Parazzoli, R.B. Greegor, K. Li, B.E.C. Koltenbah, M. Tanielian, Phys. Rev. Lett. 90 (2003) 107401.
[8] K. Aydin, K. Guven, M. Kafesaki, L. Zhang, C.M. Soukoulis, E. Ozbay, Opt. Lett. 29 (2004) 2623.
[9] M. Notomi, Phys. Rev. B 62 (2000) 10696.
[10] S. Foteinopoulou, C.M. Soukoulis, Phys. Rev. B 67 (2003) 235107.
[11] S. Foteinopoulou, E.N. Economou, C.M. Soukoulis, Phys. Rev. Lett. 90 (2003) 107402.
[12] C.Y. Luo, S.G. Johnson, J.D. Joannopoulos, J.B. Pendry, Phys. Rev. B 65 (2002) 201104.
[13] K.M. Ho, C.T. Chan, C.M. Soukoulis, Phys. Rev. Lett. 65 (1990) 3152.
[14] J. Li, L. Zhou, C.T. Chan, P. Sheng, Phys. Rev. Lett. 90 (2003) 83901.
[15] In Ref. 14, for the multilayer system an average refractive index, n_{av}, is defined as: $n_{av} = (an_A + bn_B)/(a+b)$, where $n_{A/B}$, and a/b represent the refractive index and dimensions of the constituent layers.
[16] D. Bria, B. Djafari-Rouhani, A. Akjoui, L. Dobrzynski, J.P. Vigneron, E.H. El Boudouti, A. Nouqaoui, Phys. Rev. E 69 (2004) 06613.
[17] I.V. Shadrivov, N.A. Zharova, A.A. Zharov, Y.S. Kivshar, Phys. Rev. E 70 (2004) 046615.
[18] H. Jiang, H. Chen, H. Li, Y. Zhang, S. Zhu, Appl. Phys. Lett. 83 (2003) 5386–5388.
[19] L. Wu, S. He, H. Chen, Opt. Expr. 11 (2003) 1283.
[20] L. Wu, S. He, L. Shen, Phys. Rev. B 67 (2003) 235103.
[21] D.R. Fredkin, A. Ron, Appl. Phys. Lett. 81 (2002) 1753.
[22] L.-G. Wang, H. Chen, S.-Y. Zhu, Phys. Rev. B 70 (2004) 245102.
[23] J.N. Winn, Y. Fink, S. Fan, J.D. Joannopoulos, Opt. Lett. 23 (1998) 1573.
[24] If $r_{A/B} < 0$ then for consistency $\theta_{A/B}$ must be chosen negative. Essentially parameter β remains positive for any case.
[25] P. Yeh, A. Yariv, C.S. Hong, J. Opt. Soc. Am. 67 (1977) 423.
[26] P. Yeh, Optical waves in layered media, Wiley Series in Pure and Applied Optics, 1988.
[27] The entire multilayer system is embedded in air. Such cases cannot be treated with the equations given in Section 2, since they require the embedding medium to be the same as one of the constitutive layers. Instead, we determine the transfer matrix [M] for the entire system, by applying the relevant continuity conditions for the tangential components of electric and magnetic field. Subsequently, we perform the matrix multiplication for the resulting expression numerically. Then, the transmission T through the total multilayer system is: $T = 1 - |M_{21}/M_{11}|^2$.
[28] If an incident wave falls on or above the TIR condition, then k_{Ax} is zero or imaginary. So, $\sin(k_{Ax}a)$ in Eq. (6) can become zero only in the case k_{Ax} is zero.
[29] If we are above the TIR, then $k_{Ax}^2 < 0$ (k_{Bx} is always positive since waves come from medium B). Notice: Diff $Z = Z_{A/B} - Z_{B/A} = \frac{\mu_A \mu_B}{k_{Ax} k_{Bx}} \left(\frac{k_{Ax}^2}{\mu_A^2} - \frac{k_{Bx}^2}{\mu_B^2}\right)$. Consequently, Diff $Z \neq 0$. In the same way we get Diff $Y = Y_{A/B} - Y_{B/A} \neq 0$.
[30] S. Linden, C. Enkrich, M. Wegener, J. Zhou, T. Koschny, C.M. Soukoulis, Science 19 (2004) 306.